

Cooling of Ultradegenerate Quark Matter

Kai Schwenzer*

University of Graz

E-mail: kai.schwenzer@uni-graz.at

We study the cooling of compact star cores due to neutrino emission from ungapped quark modes within an effective theory for magnetic interactions at high density. As shown recently the relevant low energy dynamics is semi-perturbative even for realistic couplings of order one due to a systematic expansion scheme in $(\omega/m)^{1/3}$, where ω is the energy and m the screening scale. We find that the characteristic T^6 behavior of the neutrino emissivity remains valid even when the strong coupling is not small. In the weak coupling limit the results shows a non-Fermi liquid low temperature enhancement.

*29th Johns Hopkins Workshop on current problems in particle theory: strong matter in the heavens
1-3 August
Budapest*

*Speaker.

1. Introduction

Despite a wealth of proposed phases [1, 2, 3, 4, 5, 6, 7], the actually realized form of matter at high density still presents a largely unsolved puzzle. Since compact stars constitute the most dense form of matter in nature they could provide detailed information on its specific properties. An important feature of compact stars in this regard is that they represent relatively cold objects. The matter in their cores - which may consist of quarks if the density is sufficiently high - becomes ultradegenerate basically within the first minutes after the formation of the proto-neutron star, as the temperature drops to values of the order $T/\mu \sim 1/1000$ and decreases further at later times. Therefore, only low energy modes in the immediate vicinity of the Fermi surface are present and determine many properties of the star.

As argued recently the dynamics of low energy modes in dense matter is strongly restricted due to the special kinematics of unscreened magnetic gauge interactions and the corresponding scaling relations near the Fermi surface. In particular, there exists a systematic low energy expansion for ungapped infrared modes in powers of $(\omega/m)^{1/3}$, where ω is the characteristic energy scale of the considered process and m is the screening scale [8]. This perturbative approach does not rely on the weak coupling limit which is only realized at densities that are much larger than the densities that can be achieved deep inside a neutron star. The low energy dynamics is described by an effective theory for unscreened magnetic interactions which involves a few low energy constants that parametrize the unknown ultraviolet physics of strongly coupled modes away from the Fermi surface.

An important source of information obtained from the observation of compact stars is their cooling behavior [9, 10]. For the first $\sim 10^5$ years after the star is born neutrino emission from the bulk is the most efficient energy loss mechanism. The neutrino emission from fully gapped phases, like the CFL-phase [2] realized at asymptotically large densities, is exponentially suppressed [11] and thereby hardly detectable against a background from hadronic processes. In contrast, the neutrino emission from ungapped quark modes via the direct URCA process presents presumably the most efficient cooling mechanism with a neutrino emissivity $\varepsilon \sim T^6$ [12]. Since other known mechanisms [13, 14, 15, 16] including those of hadronic processes yield an emissivity that is either suppressed by higher powers of T or other small factors, this cooling scenario could provide a clear signature for ungapped quark matter in astrophysical observations.

In this paper we show that due to the low temperatures present in a compact star the neutrino emissivity can be computed in a low energy expansion and has the weak coupling form even in the physical case where the coupling is not small. Moreover, the emissivity is further enhanced by unscreened magnetic interactions and has the dependence $\varepsilon \sim T^6 \log^2 T$ at small temperature, as shown recently [17].

2. Low energy dynamics in dense matter

We will start with an analysis of correlation functions at low energies $\omega \ll m$ which are required for the subsequent computation of astrophysical observables. This will be done within an effective theory for the unscreened low energy dynamics at high density valid below an UV cutoff scale $\Lambda < m$. The dominant dynamical mechanism that influences the form of the low energy

$g(\Lambda)$	m	$\delta\mu$	Z_{\perp}	v_F	Z_{\parallel}	V_{ZS}^1	V_{BCS}^3
$g(\mu)$	$\frac{g}{2\pi} N_f^{1/2} \mu$	$\frac{g^2}{3\pi^2} \mu$	1	$1 - \frac{g^2}{6\pi^2} \log\left(\frac{2^{5/2} e^{2/3} m}{\pi\Lambda}\right)$	$1 + \frac{g^2}{9\pi^2} \log\left(\frac{2^{5/2} m}{\pi\Lambda}\right)$	$\frac{2g^2}{9} \log\left(\frac{2^{5/2} m}{\pi\Lambda}\right)$	$\frac{g^2}{9} \log\left(\frac{2^{11/2} \mu^6}{\pi m^5 \Lambda}\right)$

Table 1: Leading order expressions for the low energy constants appearing in the effective Lagrangian for magnetic modes in the weak coupling limit.

excitations stems from hard dense quark loops (HDLs) [18] in purely gluonic correlation functions. Although these fluctuations involve hard momenta in a narrow interval around the Fermi surface, they are sensitive to soft energies and thereby induce infrared non-analyticities. However, as far as the fluctuations above Λ do not change the symmetries of the groundstate all other corrections should be analytic even at strong coupling. As argued by Hong [19] this fermionic part of the effective action allows a low energy expansion in derivatives over the large scale μ . Thereby the effective Lagrangian reads to lowest order

$$\begin{aligned} \mathcal{L} = & \psi_{\pm\vec{v}}^{\dagger} \left(iZ_{\parallel} v_{\pm} \cdot D - Z_{\perp} \frac{D_{\perp}^2}{2\mu} + \delta\mu \right) \psi_{\pm\vec{v}} - \frac{1}{4} G_{\mu\nu}^a G_a^{\mu\nu} + \mathcal{L}_{\text{HDL}} \\ & + \frac{V_{\text{ZS}}^{\Gamma}}{\mu^2} (\psi_{\vec{v}}^{\dagger} \Gamma \psi_{\vec{v}}) (\psi_{\vec{v}}^{\dagger} \Gamma \psi_{\vec{v}}) + \frac{V_{\text{BCS}}^{\Gamma}}{\mu^2} (\psi_{\vec{v}}^{\dagger} \Gamma \psi_{\vec{v}}) (\psi_{-\vec{v}}^{\dagger} \Gamma \psi_{-\vec{v}}) + \dots, \end{aligned} \quad (2.1)$$

where $v_{\pm}^{\mu} = (1, \pm\vec{v})$ labels the local Fermi velocity of the fields $\psi_{\pm\vec{v}}$ which describe particles and holes with momenta $p = \pm\mu\vec{v} + l$, where $l \ll \mu$, in two opposite patches on the Fermi surface entering the only kinematically allowed interactions. We will write $l = l_0 + l_{\parallel} + l_{\perp}$ with $\vec{l}_{\parallel} = \vec{v}(\vec{l} \cdot \vec{v})$ and $\vec{l}_{\perp} = \vec{l} - \vec{l}_{\parallel}$. Suppressing a constant contribution to the pressure, the effect of quantum fluctuations above the cutoff Λ is encoded in a few "low energy constants". In particular, these are given by a shift $\delta\mu$ of the Fermi surface, the Fermi velocity $|\vec{v}|$ and the renormalization factors Z_{\parallel} and Z_{\perp} , the gauge coupling g at the scale Λ and further induced higher order parameters like the four quark couplings V_{ZS}^{Γ} and V_{BCS}^{Γ} in the forward (Zero Sound) and backward (BCS) channels. The perturbative values for these parameters are given in Tab. 1. \mathcal{L}_{HDL} denotes the HDL generating functional [20]

$$\mathcal{L}_{\text{HDL}} = -\frac{m^2}{2} \sum_{\nu} G_{\mu\alpha}^a \frac{v^{\alpha} v^{\beta}}{(\nu \cdot D)^2} G_{\mu\beta}^b. \quad (2.2)$$

This term describes screening and damping of soft gluon modes due to particle-hole pairs on the entire Fermi surface. In perturbation theory the dynamical gluon mass is given by $m^2 = N_f \alpha_s \mu^2 / \pi$ and involves the gauge coupling at the scale μ . The presence of the HDL term can also be established using renormalization group arguments [21] or effective action techniques [22].

We now analyze the dynamics of the theory governed by eq. (2.1,2.2). We first note that particle-hole loops have already been integrated out and are represented by the HDL term. The effective theory describes the interaction of particles and holes with soft gluons which do not significantly change their velocity \vec{v} . Since electric fields are screened the interaction at low energies is dominated by the exchange of magnetic gluons. Magnetic gluons are weakly damped in the kinematic

regime $|k_0| \ll |\vec{k}|$. In this regime

$$D_{ij}^{(m)}(k) = \frac{\delta_{ij} - \hat{k}_i \hat{k}_j}{k_0^2 - \vec{k}^2 + i\frac{\pi}{2}m^2|\frac{k_0}{k}|}. \quad (2.3)$$

and we observe that the propagator becomes large if

$$|\vec{k}| \sim (m^2|k_0|)^{1/3} \gg |k_0|. \quad (2.4)$$

This implies that the gluon is very far off its energy shell and not a propagating state. We will compute a general diagram by picking up the pole in the quark propagator, and integrate over the cut in the gluon propagator using the kinematics dictated by eq. (2.4). In order for a quark to absorb the large momentum carried by a gluon and stay close to the Fermi surface this momentum has to be transverse to the momentum of the quark. This means that the term $k_\perp^2/(2\mu)$ in the quark propagator is relevant and has to be kept at leading order. Equation (2.4) shows that $k_\perp^2/(2\mu) \gg k_0$ as $k_0 \rightarrow 0$. This means that the pole of the quark propagator is governed by the condition $k_{||} \sim k_\perp^2/(2\mu)$. We conclude that quark and gluon momenta scale with respect to an external energy scale ω according to

$$k_0 \sim \omega, \quad k_{||} \sim m^{\frac{4}{3}}\omega^{\frac{2}{3}}/\mu, \quad k_\perp \sim m^{\frac{2}{3}}\omega^{\frac{1}{3}}. \quad (2.5)$$

We will refer to the regime in which all momenta, including external ones, satisfy the scaling relation (2.5) as the magnetic regime. A similar regime was identified in the context of gauge theories of condensed matter systems [23]. The scaling relations (2.5) are the basis of the low energy expansion in ultradegenerate matter.

In the low energy regime propagators and vertices can be simplified even further. The quark and gluon propagators are

$$S_{\pm\bar{v}}^{\alpha\beta}(p) = \frac{i\delta_{\alpha\beta}}{Z_{||}(p_0 \mp v_F p_{||}) - Z_\perp \frac{p_\perp^2}{2\mu} + i\varepsilon \text{sgn}(p_0)}, \quad (2.6)$$

$$v_+^\mu v_\pm^\nu D_{\mu\nu}^{(m)}(k) = \mp \frac{iv_F^2}{k_\perp^2 + i\frac{\pi}{2}m^2|\frac{k_0}{k_\perp}|}, \quad (2.7)$$

and the quark gluon vertex is $gZ_{||}v_i(\lambda^a/2)$. Higher order corrections can be found by expanding the quark and gluon propagators as well as the HDL vertices in powers of the small parameter $\varepsilon \equiv \omega/m$ [21]. We observe that the transverse projector in the gluon propagator simplifies because $k_\perp \gg k_{||}$. We also note that in the magnetic regime the factor p_0 in the quark propagator can be dropped since $p_0 \ll p_{||}$. From the above scaling rules it follows that the magnetic regime is completely perturbative, i.e. graphs with extra loops are always suppressed by extra powers of $\varepsilon^{1/3}$. Quark propagators scale as $\varepsilon^{-2/3}$, gluon propagators scale as $\varepsilon^{-2/3}$, and every loop integral gives $\varepsilon^{7/3}$. The quark-gluon vertex scales as ε^0 and the HDL three-gluon vertex scales as $\varepsilon^{1/3}$. Using these results we can show that additional loops always increase the power of ε associated with the diagram.

The analysis of the cooling behavior requires the fermionic self energy as dynamical input. The one-loop diagram gives

$$\Sigma(p) = g^2 C_F \int \frac{dk_0}{2\pi} \int \frac{dk_\perp^2}{(2\pi)^2} \frac{k_\perp}{k_\perp^3 + i\frac{\pi}{2}m^2|k_0|} \int \frac{dk_{||}}{2\pi} \frac{\Theta(p_0 + k_0)}{(k_{||} + p_{||}) + \frac{Z_\perp(k_\perp + p_\perp)^2}{2Z_{||}v_F\mu} + i\varepsilon}, \quad (2.8)$$

with $C_F = (N_c^2 - 1)/(2N_c)$. This expression shows a number of interesting features. First we observe that the longitudinal and transverse momentum integrations factorize. The longitudinal momentum integral can be performed by picking up the pole in the quark propagator. The result is independent of the external momenta and only depends on the external energy. The transverse momentum integral is logarithmically divergent. We find the non-Fermi liquid correction [24]

$$\Sigma(p) = \frac{C_F \alpha_s}{3\pi} \left(\omega \log \left(\frac{\Lambda_\Sigma}{|\omega|} \right) + \omega + i \frac{\pi}{2} |\omega| \right) + O \left(\varepsilon^{\frac{5}{3}} \right), \quad (2.9)$$

where $\omega \equiv p_0$. We have absorbed the logarithmic cutoff dependence into the low energy constant Z_\parallel . In the general case this result depends on two unknown parameters g and Λ_Σ which is connected to the low energy constants by $\Lambda_\Sigma = \Lambda \exp(9\pi^2(Z_\parallel - 1)/(g^2 Z_\parallel v_F))$, where $\Lambda = 2\Lambda_\perp^3/(\pi m^2)$ is related to the transverse momentum cutoff. If in addition the coupling is small, the scale is determined by the exchange of electric gluons and we find $\Lambda_\Sigma = 2^{5/2} m/\pi$. We observe that the self energy correction is large and has to be included in the propagator whenever the energy dependence of the propagator is relevant. We showed previously that rainbow diagrams do not give corrections of the form $g^{2n} \omega \log(\omega)^n$ [25]. Eq. (2.9) shows that higher order corrections are suppressed by powers of $\varepsilon^{2/3}$.

Collecting the contributions from the tree level and loop corrections eqs. (2.1,2.9) in the effective field theory, the fermionic dispersion relation is given by

$$\omega - v_F l + \frac{\delta\mu}{Z_\parallel} + \Sigma(\omega) = 0, \quad (2.10)$$

which depends on four low energy constants that are known in the weak coupling limit Tab. 1.

The scaling arguments apply to arbitrary Green functions in the magnetic regime. Exceptions occur if the external fields have small momenta of the order of the external energy scale. This situation can occur in quark-quark scattering amplitudes or in vertex functions for external currents like the weak interaction which represents the other required correlation function for the computation of the neutrino emissivity in the next section. Consider the one-loop vertex correction for a color singlet vertex $\Gamma_\mu = e Z_\parallel v_\mu$. In the magnetic regime the graph scales like $\varepsilon^{1/3}$. In the time-like regime $p_0 - q_0 > |\vec{p} - \vec{q}|$

$$\Gamma^\mu(p, q) = e g^2 C_F \hat{v}_+^\mu \int \frac{dk_0}{2\pi} \int \frac{d^2 k_\perp}{(2\pi)^2} v_+^\rho v_+^\sigma D_{\rho\sigma}^{(m)}(k) \int \frac{dk_\parallel}{2\pi} Z_\parallel^2 S_{\bar{v}}(k+p) S_{\bar{v}}(k+q), \quad (2.11)$$

where p, q are the momenta of the external quarks. The important point is that if we combine the fermionic propagators using Fermi's trick in order to resolve the pole in the longitudinal momentum integration, the large components k_\parallel and $k_\perp^2/(2\mu)$ of the propagators cancel and the result becomes sensitive to the small scales p, q

$$S_{\bar{v}}(k+p) S_{\bar{v}}(k+q) = \frac{S_{\bar{v}}(k+p) - S_{\bar{v}}(k+q)}{S_{\bar{v}}^{-1}(p) - S_{\bar{v}}^{-1}(q) - \frac{2\vec{k}_\perp \cdot (\vec{p}_\perp + \vec{q}_\perp)}{\mu}},$$

where constant factors are suppressed. As a consequence the result is enhanced by a factor $1/\varepsilon^{1/3}$. This enhancement is analogous to the one occurring in the HDL case. In the limit $p_0 - q_0 \rightarrow 0$ the

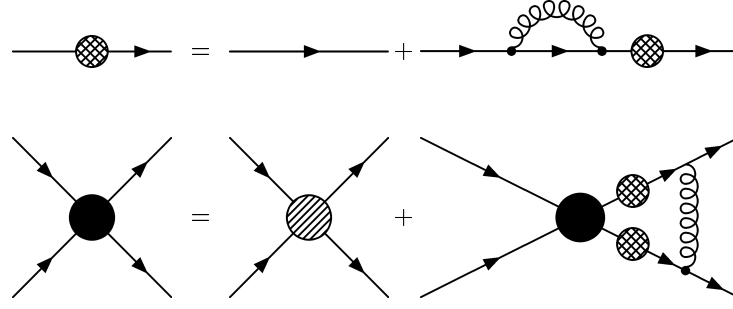


Figure 1: The complete dynamics contributing to the Dyson-Schwinger equation for the BCS kernel in the low energy limit. The dark blob represents the full scattering amplitude and the shaded blob the full propagator. An analog but independent equation is obtained for the forward channel.

$k_{||}$ integral gives a factor $\delta(p_0 - k_0)$ and the vertex correction is [26]

$$\Gamma^\mu(p, q) = \frac{eg^2}{9\pi^2} \hat{v}_+^\mu \log\left(\frac{\Lambda_{ZS}}{|\omega|}\right), \quad (2.12)$$

where $\omega = (p_0 + q_0)/2$. The logarithmic divergence was removed by adding the contribution from the four-fermion vertex in the zero sound channel. If the coupling is weak the scale inside the logarithm is again determined by electric gluon exchange. We find that in this case the scale is equal to the scale in the quark self energy.

The cancellation that occurs in the one-loop diagram repeats itself at any loop order if additional gluon ladders are added. This implies that ladder diagrams have to be summed. We also note that quark propagators in the ladders are sensitive to the small scale ω . This implies that the full fermion self energy has to be included. A detailed analysis shows that all other corrections like crossed ladders, vertex corrections, interconnections between the gluon ladders, etc. introduce extra transverse momenta and follow the scaling relations in the magnetic regime. Actually, a comprehensive study of the low energy dynamics shows that correlation functions within the effective theory can be classified completely [21]. The only other correlation functions that involve irreducible non-perturbative contributions are the four fermion vertices where a similar mechanism requires the summation of the corresponding ladder sum [8]. The non-perturbative part of the dynamics in the low energy regime is thereby described by a closed set of Dyson-Schwinger equations shown in Fig. 1.

3. Neutrino emissivity

The dominant contribution to the emission of neutrinos from ungapped quarks is given by the quark analogs of β -decay (β) and electron capture (ec)

$$d \rightarrow u + e^- + \bar{\nu}_e, \quad (3.1)$$

$$u + e^- \rightarrow d + \nu_e. \quad (3.2)$$

It is straightforward to introduce weak interactions into the effective theory. The charged current interaction is given by

$$\mathcal{L} = \frac{g_2}{\sqrt{2}} \cos\theta_c \psi^\dagger \tau^\pm \nu \cdot W^\mp \psi \quad (3.3)$$

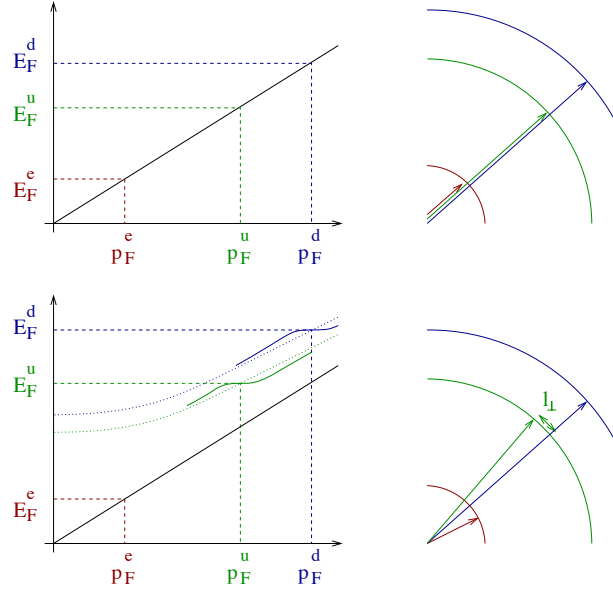


Figure 2: Kinematics for the quark direct Urca process. In a free quark gas (upper panel) energy momentum conservation forces all momenta to be collinear. If Fermi liquid corrections are taken into account (lower panel) the outgoing quark has a non-zero transverse momentum $l_{\perp}^2 \sim \alpha_s \mu_e^2$. The dashed dispersion relations give the HDL result whereas the solid lines show the change when non-Fermi liquid corrections are included. These lead to a flattening of the dispersion relation in the vicinity of the Fermi surface.

where $\cos \theta_c$ is the Cabbibo angle and g_2 is related to the Fermi coupling by $G_F/\sqrt{2} = g_2^2/(8M_W^2)$. The dependence on the Cabbibo angle suppresses the processes involving the strange quark [12]. Therefore we will restrict our analysis to $N_f = 2$ massless quarks. We have seen in the previous section that almost collinear gluon exchanges can generate large logarithmic corrections to both the fermion self energy and the vertex correction in the time-like regime. In particular, the coefficients of the respective logarithms are exactly equal. Since the kinematics in the case of the neutrino processes eq. (3.1,3.2) is timelike the logarithms cancel and the renormalized effective weak coupling remains unchanged.

The neutrino emissivity is given by the total energy loss due to neutrino emission averaged over the initial quark helicities and summed over the final state phase space and helicities

$$\begin{aligned} \varepsilon \equiv N_c \frac{1}{2} \sum_{\sigma_u, \sigma_d, \sigma_e} \int \frac{d^3 p_d}{(2\pi)^3} \frac{1}{2E_d} \int \frac{d^3 p_u}{(2\pi)^3} \frac{1}{2E_u} \int \frac{d^3 p_e}{(2\pi)^3} \frac{1}{2E_e} \int \frac{d^3 p_\nu}{(2\pi)^3} \frac{1}{2E_\nu} E_\nu \\ \cdot \left(|M_\beta|^2 (2\pi)^4 \delta^{(4)}(p_d - p_u - p_e - p_\nu) n(p_d) (1 - n(p_u)) (1 - n(p_e)) \right. \\ \left. + |M_{ec}|^2 (2\pi)^4 \delta^{(4)}(p_u + p_e - p_d - p_\nu) n(p_u) n(p_e) (1 - n(p_d)) \right) \end{aligned} \quad (3.4)$$

where E_i, p_i represent the full energies and momenta instead of the corresponding quantities relative to the Fermi surface appearing in the effective theory. The weak matrix element for the β and ec processes is given by

$$\frac{1}{2} \sum_{\sigma_u, \sigma_d, \sigma_e} |M_{\beta/ec}|^2 = 64 G_F^2 \cos^2 \theta_c p_F^2 (v \cdot p_e)(v \cdot p_\nu), \quad (3.5)$$

where p_e, p_ν are the momenta of the electron and the neutrino. Weak processes establish β equilibrium in the star. In three flavor quark matter with a massive strange quark the resulting electron chemical potential is small. In the following we shall assume that $(T \sim E_\nu) \ll (\mu_e \sim E_e) \ll p_F$. This assumption is appropriate in all cases except during the first few seconds of the proto-neutron star evolution.

In this case we can neglect the neutrino energy and momentum when applying the energy-momentum conservation relation to the matrix element. As a consequence we find $(v \cdot p_\nu) \simeq E_\nu$ after averaging over the direction of the outgoing neutrino. The matrix element is mainly determined by the factor $(v \cdot p_e)$. To leading order in the effective theory the weak decay is exactly collinear and $(v \cdot p_e) = (E_e - v_F l_e) = 0$ up to terms of order $O(T/\mu_e)$, see Fig. 2. The modification of the dispersion relation due to interactions opens phase space for the URCA processes. The leading effect which makes the integral finite comes from Fermi liquid corrections, whereas non-Fermi liquid corrections only appear in the phase space integral. To leading order in T/μ the sum of the rates for electron capture and β decay is given by

$$\varepsilon \approx \frac{3G_F^2 \cos^2 \theta_c}{2\pi^5} T^6 \int_{-\infty}^{\infty} dx_d \int_{-\infty}^{\infty} dx_u \int_0^{\infty} dx_\nu x_\nu^3 n(x_d) n(-x_u) n(x_u - x_d + x_\nu) \cdot \left[\frac{p(E_d)}{E_d} \frac{\partial p(E_d)}{\partial E_d} \frac{p(E_u)}{E_u} \frac{\partial p(E_u)}{\partial E_u} (p(E_u)^2 - E_u^2 - p(E_d)^2 + E_d^2) \right]_{E_i \rightarrow \mu_i + T x_i}. \quad (3.6)$$

In the considered case $T \ll \mu$ the distribution functions cut off the integration at scales of the order T which allows the application of the low energy expansion. Thereby the expression in the square brackets is determined by the quark dispersion relation given in eq. (2.10) and can be expressed by the low energy constants. In the general case when the coupling is not small the integral cannot be done analytically but has to be performed numerically which would require values for the unknown low energy constants. The important point is, however, that in the considered case the leading term arising from the bracket depends only logarithmically on the temperature and thereby does not change the generic T^6 behavior.

In weak coupling, terms of $O(\alpha_s (\alpha_s \log(T))^n)$ with $n = 0, 1, 2$ are independent of $\log(x_i)$ and leave the integral

$$\int_{-\infty}^{\infty} dx_d \int_{-\infty}^{\infty} dx_u \int_0^{\infty} dx_\nu x_\nu^3 n(x_d) n(-x_u) n(x_d - x_u + x_\nu) = \frac{457\pi^6}{5040}. \quad (3.7)$$

In this case the neutrino emissivity from the quark direct Urca process reads at leading order in T/μ

$$\varepsilon \approx \frac{457}{630} G_F^2 \cos^2 \theta_c \alpha_s \mu_q^2 \mu_e T^6 \left(1 + \frac{C_F \alpha_s}{3\pi} \log \left(\frac{e\Lambda_\Sigma}{T} \right) \right)^2. \quad (3.8)$$

The first term is the standard result by Iwamoto [12], and the logarithmic terms are non-Fermi liquid corrections. We note that these terms have to be included because at very low temperature $\alpha_s \log(T)$ becomes large compared to one. We also note that if the scale inside the logarithm is on the order of the screening scale $\sim g\mu$, then $\alpha_s(\mu) \log(\Lambda/T)$ stays finite in the limit $\mu \rightarrow \infty$ at fixed T .

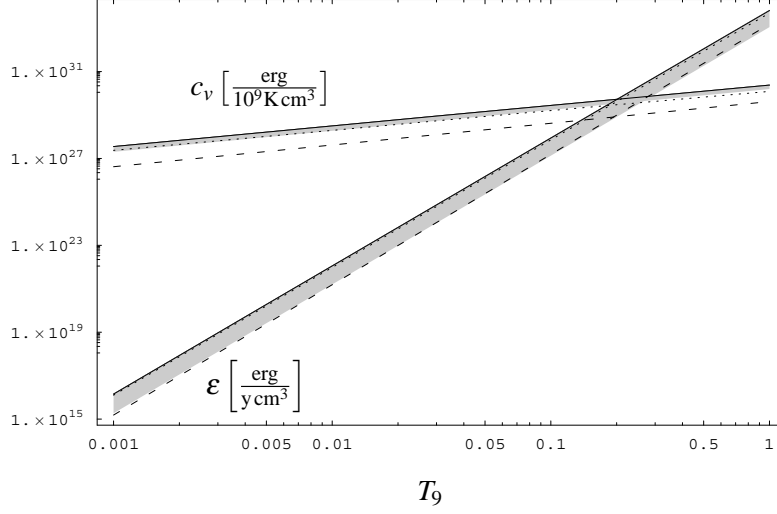


Figure 3: Neutrino emissivity ε and specific heat c_v of quark matter. The dashed line shows the Fermi liquid results and the dotted lines show the anomalous corrections. The solid line gives the sum of the two contributions and the gray band shows an estimate of the uncertainties.

4. Compact star cooling

In this section we wish to study the impact of non-Fermi liquid effects on the cooling history of an isolated quark phase in the weak coupling limit. Our aim is not to provide a thorough analysis of the cooling behavior of an actual quark or hybrid star, but to give a numerical estimate of the size of the non-Fermi liquid corrections. The thermal evolution of the star is governed by the neutrino emissivity, the specific heat and the thermal conductivity. Non-Fermi liquid corrections to the specific heat were initially considered by Holstein et al. [27] in the case of QED. The calculation was recently refined and extended to QCD by Ipp et al. [28]. They find

$$c_v = \frac{N_c N_f}{3} \mu_q^2 T \left(1 + \frac{C_F \alpha_s}{3\pi} \log \left(\frac{\Lambda_c}{T} \right) \right), \quad (4.1)$$

where the first term is the free gas result and the second term is the non-Fermi liquid correction. Ipp et al. also determined the scale inside the logarithm as well as fractional powers of T . From the complete $O(\alpha_s)$ result we find $\Lambda_c \simeq 0.28m$ which is substantially smaller than the effective scale $e \cdot \Lambda_\Sigma \simeq 4.98m$ found for the self energy.

The thermal conductivity of degenerate quark matter was studied by Pethick and Heiselberg [29]. Their result suggests that equilibration is fast and that the quark phase is isothermal. In this case the cooling behavior is governed by

$$\frac{\partial u}{\partial t} = \frac{\partial u}{\partial T} \frac{\partial T}{\partial t} = c_v(T) \frac{\partial T}{\partial t} = -\varepsilon(T), \quad (4.2)$$

where u is the internal energy, t is time and we have assumed that there is no surface emission. Without non-Fermi liquid effects we have $\varepsilon \sim T^6$ and $c_v \sim T$. In this case the temperature scales as $T \propto 1/t^{1/4}$. With logarithmic corrections included there is no simple analytic solution and we have studied eq. (4.2) numerically.

We take the quark chemical potential to be $\mu_q = 500$ MeV corresponding to densities $\rho_B \approx 6\rho_0$ where ρ_0 is nuclear matter saturation density. We note that both c_v and ε are proportional to μ^2 and the main dependence of the cooling behavior on μ cancels. We evaluate the strong coupling constant using the one loop renormalization group solution at a scale μ . We take the scale parameter to be $\Lambda_{QCD} = 250$ MeV which gives $\alpha_s \simeq 1$ at $\mu = 500$ MeV. It is clear that the naive use of perturbation theory is in doubt if the coupling is this large. In practice we estimate the uncertainty by varying α_s between 1 and 0.4 which is the value used by Iwamoto [12]. We take the weak coupling result for the scale in the logarithms and assess the uncertainty by varying Λ within a factor of 2. Finally, we took the initial temperature to be $T_0 = 15$ MeV.

The electron chemical potential is determined by the requirements of charge neutrality and β -equilibrium. In a non-interacting quark gas we find $\mu_e \simeq m_s^2/(4p_F)$. With a strange quark mass $m_s = 150$ MeV this relation gives $\mu_e \approx 11$ MeV. This result, however, is very sensitive to interactions. To first order in α_s the chemical potential for a massive strange quark is [30]

$$\mu_s = E_{F_s}^0 + \frac{2\alpha_s}{3\pi} \left(p_{F_s} - \frac{3m_s^2}{E_{F_s}^0} \log \left(\frac{p_{F_s} + E_{F_s}^0}{m_s} \right) \right) \quad (4.3)$$

where $E_{F_s}^0 = \sqrt{p_{F_s}^2 + m_s^2}$. The important point is that the $O(\alpha_s m_s^2)$ term is negative and enhanced by a large logarithm $\log(p_F/m_s)$. The sign is related to the fact that the correlation energy changes sign in going from the relativistic to the non-relativistic limit.

Equation (4.3) implies that the strange quark chemical potential can become equal to or even smaller than the up quark chemical potential. To leading order in m_s^2/p_F^2 the electron chemical potential is given by

$$\mu_e \simeq \frac{m_s^2}{4p_F} \left(1 - \frac{4\alpha_s}{\pi} \log \left(\frac{2p_F}{m_s} \right) \right). \quad (4.4)$$

For the values of the parameters given above this equation gives a negative electron chemical potential $\mu_e \approx -14$ MeV. In this case the quark phase contains a Fermi sea of positrons and the quark direct Urca process is

$$u \rightarrow d + e^+ + \nu \quad , \quad d + e^+ \rightarrow u + \bar{\nu}. \quad (4.5)$$

The neutrino emissivity is again governed by eq. (3.8) where μ_e has to be replaced by $-\mu_e$. We observe that despite the large correction to μ_e the emissivity is not strongly affected. The large variation in μ_e when perturbative corrections are included implies, however, that the electron chemical potential is very uncertain. In particular, there is a possibility that μ_e is much smaller than $m_s^2/(4p_F)$. If $\alpha_s \mu_e < T$ then the neutrino emissivity is no longer proportional to $\alpha_s \mu_e T^6$ but to T^7 [31]. In the following we shall use the value $\mu_e = 14$ MeV corresponding to interacting quarks. In Fig. 3 we show the temperature dependence of both the neutrino emissivity and the specific heat (solid) compared to the Fermi liquid result (dashed). The gray band shows an estimate of the uncertainties which are dominated by the uncertainty in the value of the strong coupling. For both c_v and ε the anomalous logarithmic terms (dotted) dominate in the relevant temperature range and exceed the Fermi liquid result considerably. The cooling behavior is controlled by the ratio ε/c_v . Since $\varepsilon \sim \log^2(T)$ and $c_v \sim \log(T)$ this ratio is logarithmically enhanced. However, because the temperature at late times scales roughly as the fourth root of the numerical coefficient in ε/c_v this logarithmic enhancement only translates into a modest reduction of the temperature. This can be seen in more

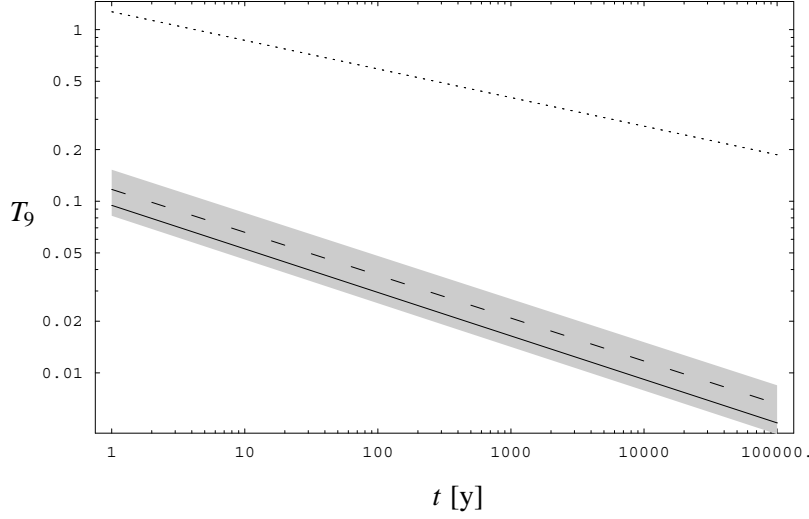


Figure 4: Cooling behavior of ungapped quark matter. We show the temperature T_9 in units of 10^9 K as a function of the age of the star in years. The dashed line shows the Fermi liquid result whereas the solid line gives the result including non-Fermi liquid effects with the estimated uncertainty range. Although the non-Fermi liquid corrections to both the specific heat and the neutrino emissivity are significant, there is only a modest reduction in the temperature at late times. However, for both cases the cooling of quark matter is considerably faster than the cooling of neutron matter via the modified Urca process given by the dotted line.

detail in Fig. 4. We observe that compared to the Fermi liquid result (dashed) the non-Fermi liquid effects (solid) lead to a reduction of the temperature at late times which is nearly independent of time. The magnitude of the effect is on the order of 20%. For comparison, we also show the cooling behavior of normal nuclear matter via the modified Urca process $n + n \rightarrow n + p + e^- + \bar{\nu}$ [13]. We have chosen the same density and initial temperature and the effective baryon masses given in [10]. We clearly see the difference between the fast $\sim T^6$ quark direct Urca process and the slow $\sim T^8$ modified Urca process.

5. Summary and Discussion

In this work, we have discussed the influence of ungapped quark modes on the cooling behavior of compact stars. We find that the functional form and in particular the temperature dependence of the neutrino emissivity found in the weak coupling limit generalizes to the physical case where the coupling is of order one. This result is obtained within an independent low energy expansion and should be valid basically during the entire cooling process except for the initial part. The low energy expansion shares many features with the ordinary weak coupling expansion and depends on only a few unknown low energy constants whose size should roughly be given by the perturbative values. We expect a similar qualitative agreement between the weak coupling and the low energy expansion for the case of the specific heat. A more precise result will require a detailed study of both the emissivity and the specific heat within the effective low energy theory.

In the weak coupling limit non-Fermi liquid effects lead to a logarithmic enhancement in both the neutrino emissivity and the specific heat. The net result of these two effects is a mild logarithmic

enhancement in the cooling rate. As our rate is even larger than the Iwamoto rate we confirm and sharpen earlier bounds on the existence of ungapped quark matter in neutron stars [32]. More quantitative statements will require detailed studies of realistic models in which the quark core is in contact with a hadronic phase or an atmosphere which is beyond the scope of the present paper.

References

- [1] D. Bailin and A. Love, Phys. Rept. **107**, 325 (1984); M. Alford, K. Rajagopal and F. Wilczek, Phys. Lett. **B422**, 247 (1998) [hep-ph/9711395]; R. Rapp, T. Schäfer, E. V. Shuryak and M. Velkovsky, Phys. Rev. Lett. **81**, 53 (1998) [hep-ph/9711396].
- [2] M. G. Alford, K. Rajagopal and F. Wilczek, Nucl. Phys. B **537**, 443 (1999) [hep-ph/9804403].
- [3] T. Schäfer, Phys. Rev. D **62** (2000) 094007 [hep-ph/0006034]; A. Schmitt, Q. Wang and D. H. Rischke, Phys. Rev. D **69**, 094017 (2004) [nucl-th/0311006].
- [4] M. Alford, J. Bowers and K. Rajagopal, Phys. Rev. D **63**, 074016 (2001) [hep-ph/0008208].
- [5] P. F. Bedaque and T. Schafer, Nucl. Phys. A **697** (2002) 802 [hep-ph/0105150].
- [6] I. Shovkovy and M. Huang, Phys. Lett. B **564**, 205 (2003) [hep-ph/0302142]; M. Alford, C. Kouvaris and K. Rajagopal, Phys. Rev. Lett. **92**, 222001 (2004) [hep-ph/0311286].
- [7] T. Schafer, Phys. Rev. Lett. **96** (2006) 012305 [hep-ph/0508190].
- [8] T. Schäfer and K. Schwenzer, preprint, hep-ph/0512309.
- [9] C. J. Pethick, Rev. Mod. Phys. **64**, 1133 (1992); D. G. Yakovlev and C. J. Pethick, Ann. Rev. Astron. Astrophys. **42**, 169 (2004) [astro-ph/0402143]; D. Page, U. Geppert and F. Weber, preprint, astro-ph/0508056.
- [10] D. Page, J. M. Lattimer, M. Prakash and A. W. Steiner, preprint, astro-ph/0403657.
- [11] P. Jaikumar and M. Prakash, Phys. Lett. B **516**, 345 (2001) [astro-ph/0105225]; P. Jaikumar, M. Prakash and T. Schäfer, Phys. Rev. D **66** (2002) 063003 [astro-ph/0203088]; S. Reddy, M. Sadzikowski and M. Tachibana, Nucl. Phys. A **714**, 337 (2003) [nucl-th/0203011].
- [12] N. Iwamoto, Phys. Rev. Lett. **44**, 1637 (1980).
- [13] B. L. Friman and O. V. Maxwell, Astrophys. J. **232** (1979) 541.
- [14] O. Maxwell, G. E. Brown, D. K. Campbell, R. F. Dashen and J. T. Manassah, Astrophys. J. **216** 77 (1977).
- [15] E. Flowers, M. Ruderman and P. Sutherland, Astrophys. J. **205**, 541 (1976).
- [16] J. M. Lattimer, M. Prakash, C. J. Pethick and P. Haensel, Phys. Rev. Lett. **66**, 2701 (1991).
- [17] T. Schäfer and K. Schwenzer, Phys. Rev. D **70** (2004) 114037 [astro-ph/0410395].
- [18] E. Braaten and R. D. Pisarski, Nucl. Phys. B **337** (1990) 569.
- [19] D. K. Hong, Phys. Lett. B **473**, 118 (2000) [hep-ph/9812510]; Nucl. Phys. B **582**, 451 (2000) [hep-ph/9905523];
- [20] E. Braaten and R. D. Pisarski, Phys. Rev. D **45**, 1827 (1992).
- [21] T. Schäfer and K. Schwenzer, in preparation.
- [22] P. T. Reuter, Q. Wang and D. H. Rischke, Phys. Rev. D **70**, 114029 (2004) [nucl-th/0405079].

- [23] J. Polchinski, Nucl. Phys. B **422**, 617 (1994); C. Nayak and F. Wilczek, Nucl. Phys. B **430**, 534 (1994).
- [24] C. Manuel, Phys. Rev. D **62**, 076009 (2000) [hep-ph/0005040]; A. Gerhold and A. Rebhan, Phys. Rev. D **71** (2005) 085010 [hep-ph/0501089].
- [25] T. Schäfer and K. Schwenzer, Phys. Rev. D **70**, 054007 (2004) [hep-ph/0405053].
- [26] W. E. Brown, J. T. Liu and H. C. Ren, Phys. Rev. D **62**, 054013 (2000) [hep-ph/0003199].
- [27] T. Holstein, A. E. Norton, P. Pincus, Phys. Rev. **B8**, 2649 (1973).
- [28] A. Ipp, A. Gerhold and A. Rebhan, Phys. Rev. D **69**, 011901 (2004) [hep-ph/0309019]; A. Gerhold, A. Ipp and A. Rebhan, Phys. Rev. D **70**, 105015 (2004) [hep-ph/0406087].
- [29] H. Heiselberg and C. J. Pethick, Phys. Rev. D **48**, 2916 (1993).
- [30] B. Freedman and L. D. McLerran, Phys. Rev. D **17**, 1109 (1978); R. C. Duncan, S. I. Shapiro and I. Wasserman, Astrophys. J. **267**, 358 (1983).
- [31] A. Burrows, Phys. Rev. Lett. **44**, 1640 (1980).
- [32] D. Blaschke, H. Grigorian and D. N. Voskresensky, Astron. Astrophys. **368**, 561 (2001) [astro-ph/0009120]; D. Page, M. Prakash, J. M. Lattimer and A. Steiner, Phys. Rev. Lett. **85**, 2048 (2000) [hep-ph/0005094]; M. Prakash, J. M. Lattimer, J. A. Pons, A. W. Steiner and S. Reddy, Lect. Notes Phys. **578**, 364 (2001) [astro-ph/0012136].